

# CTMP Process Optimization Part I: Internal and External Variables Impact on Refiner Conditions

Anders Karlström\*, Jan Hill\*\*, \*Chalmers University of Technology, Göteborg, Sweden, \*\*QualTech AB, Tyringe, Sweden

---

**KEYWORDS:** Modeling, CTMP, energy efficiency, pulp consistency, fiber residence time, fiber-to-bar interaction, temperature profile, motor load distribution

**SUMMARY:** In this paper, internal variables (e.g. temperature, consistency, fiber residence time, backward flowing steam and forces acting upon the chips and pulp) are introduced and defined as physical states obtained in different parts of the refining zones. In short, they differ from the traditional external variables (e.g. dilution water feed rate, specific energy and plate clearance) which are not available as distributed variables from refining zone measurements.

The internal variables can be seen as the backbone of physical models and we illustrate that based on a model for a CD-82 refiner. It is shown that such a model can be used for on-line implementation of soft sensors for advanced process control. Of special interest are the fiber residence time and consistency profiles in the flat and conical zones, which are the internal variables in focus in this study as they are directly linked to pulp and handsheet property development.

It is also shown that the refining segment pattern affects the temperature profile, which must be considered vital in the modeling efforts. It is particularly interesting to study how the segment parameters in terms of the distributed width of the bars and grooves together with the segment taper affect the back-flowing steam, the cross-sectional area and thereby the fiber residence time.

To illustrate the capability to use a modeling strategy it is shown how to reach a 40% reduction in specific energy without violating the pulp properties studied.

---

## ADDRESSES OF THE AUTHORS:

**Anders Karlström** ([anderska@chalmers.se](mailto:anderska@chalmers.se)), Sweden

**Jan Hill** ([jan.hill@qtab.se](mailto:jan.hill@qtab.se)), Sweden

**Corresponding author: Anders Karlström**

---

Several approaches have been proposed over the years to describe how to find proper operating points for good enough pulp quality and minimized energy consumption in refining processes. Most papers dealing with refiner optimization and control confine themselves to discussing the topic either with the perspective of an individual refiner or an individual TMP production line, see Hill et al. (1979), Johansson et al. (1980), Dahlqvist and Ferrari (1981), Oksum (1983), Honkasalo et al. (1989), Hill et al. (1993), Berg (2005), Eriksson (2005) and Eriksson (2009).

During the late 1980s, Miles and May (1990, 1991) derived a theoretical model of the pulp flow behavior in the refining zone of a high consistency (HC) refiner. A theory became widely used and increased the understanding of refining to some extent. The approach was to determine the radial pulp velocity and residence time based on calculations of the forces that affect the

flow conditions. The number of fiber impact per bar was derived from this model.

Even though the fiber residence time is one of the most important variables in controlling refining phenomena, our knowledge of it is still quite diffuse. Harkonen et al. (1999) used radioactive tracers to gain more insight into the distribution of fibers and the residence time in the refining zone. They found that the average fiber residence time was affected strongly by the mixing zone before the steam turning point. They also found that after the fibers have passed this position, the average residence time is rather small, see Harkonen et al. (2003). In general, the average fiber residence time is assumed to be less than 1-2 seconds and is strongly affected by the refining segment design and type of refiner.

Miles and May (1990, 1991) introduced the concept of refining intensity, which was defined as the ratio between the specific energy (i.e. the relation between motor load and the assumed production rate) and the number of fiber-to-bar interactions (or the fiber residence time), see Kure (1999). Miles and May (1990, 1991) used unidirectional segments, where the idea was to define a scalar that describes the bar-to-fiber impact estimated for the entire refining zone, see further Strand et al. (1993) and Murton et al. (2002).

Sabourin et al. (2001) claimed that the model derived by Miles and May (1990, 1991) is not suitable for practical use since it has too many unknown parameters and variables. One example was the friction coefficients introduced to describe the interaction between the refining segment surface and the pulp. Isaksson et al. (1997) had shown this earlier and concluded that the proposed friction coefficients are far from the values estimated in full-scale refiners and that the coefficients varied dramatically for different refining conditions.

To this time, process models, based on first principals, have been used off-line for analysis, see Karlström and Eriksson (2014a,b,c,d) and Karlström and Hill (2014a,b and 2015a,b). One reason why the implementation of such models on-line has taken such a long time is that the model complexity sometimes itself introduces barriers. Another reason is that these models produce a huge amount of data that must be handled in real-time.

This paper presents a theoretical model where a complete refiner including systems descriptions for inlet mixing zones, refining zones and outlet mixing zones are considered. The model copes with real-time process changes and is assumed to be used in future on-line applications.

This paper focuses on the description of the interplay between internal variables (e.g. temperature, consistency and fiber residence time) and external variables (e.g. dilution water feed rate, specific energy and plate clearance) from a modeling perspective. The distinction between internal and external variables as indicated

above was introduced by Karlström and Isaksson (2009) and further developed in Karlström et al. (2015 and 2016a,b). It was shown that using internal variables instead of external variables to find proper piece-wise linear models, estimating pulp and handsheet properties, gave a better opportunity to handle inherent non-linearities in the process. These results were to some extent not expected, as the major efforts to find models of pulp and handsheet properties had thus far been based on external variables as independent variables, see Strand (1996), Strand and Grace (2014) and Lehtonen et al. (2014).

This paper is the first in a series of three consecutive papers. The idea is to broaden the discussion of how to use more sophisticated refining zone measurements in combination with a refining model based on first principals to find relevant variables in analyzing pulp and handsheet properties.

Data from a full-scale CTMP production line (CD82-refiner) will be used to illustrate the need to implement physical models on-line for process optimization.

## Material and methods

Several attempts to model refining processes have been made after Miles and Mays' (1990, 1991) contributions. Berg (2005), Karlström et al. (2005), Eriksson (2009) and Karlström et al. (2008) introduced spatial temperature measurements inside the refining zone to span the material and energy balances. This led to the possibility to span the distributed work as well, see Karlström (2013).

The flow pattern in the refining zone is set by three physical states (chips/fibers ( $m_1$ ), water ( $m_2$ ) and vapor ( $m_3$ )) that must be considered simultaneously. The steam generated in the refining zone is commonly assumed to be saturated, i.e. the pressure is a function of the temperature and vice versa, regardless of which type of high-consistency refiner is studied.

From a modeling perspective, it is important that the physical properties are available at different radial positions and scales as these variables are dependent on e.g. type of refining segments and actual process conditions. It is also important that the model can handle the energy input (motor load) as a distributed work in the refining zone from a macro-scale perspective.

Karlström and Eriksson (2014a) also introduced plate gap clearance to estimate the distributed viscosity profile in a CD-82 refiner, see Fig. 1. This expansion formed the "extended entropy model," which was a set of material and energy balances for one refining zone.

The reason why the model refers to the entropy instead of the enthalpy is that the entropy generation

$$dS(r) = \frac{dE(r)}{T(r)}$$

is introduced as an important variable to distinguish between thermodynamic work given by the change in enthalpy and defibration/fibrillation work. Thus,  $dE$

refers to the energy dissipated and  $T$  is the absolute temperature.

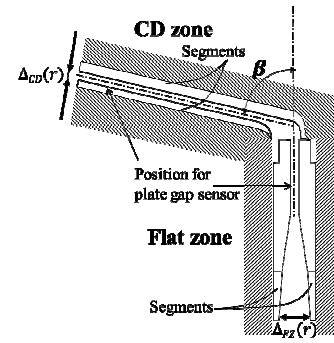


Fig. 1: A schematic drawing of the refining zones in a CD refiner. The vertical flat zone (FZ) is directly linked to the conical zone (CD) via an expanding point.

In former model assumptions (May and Miles (1990)) a pure enthalpy balance was considered,  $dH=dE$ , where  $dH$  is the enthalpy generation, which did not consider the irreversible work related to the fiber development, i.e. the entropy generation,  $dS$ , in an infinitesimal control volume is assumed to be given by the expression for the viscous dissipation,  $\delta$  (Bird et al. 1960).

$$dS(r) = \frac{\delta(r)}{T(r)} \Delta(r) 2\pi r dr$$

where

$$\delta(r) = \mu \left( \frac{r\omega}{\Delta(r)} \right)^2 = \frac{w_R(r)}{\Delta(r)}$$

Thus it will be important to measure both the temperature profile  $T(r)$  and the plate gap profiles  $\Delta(r)$  in the refining zone, together with the entire motor load  $w_R$ , when deriving the dynamic viscosity  $\mu(r)$ .

Measuring the temperature profile is important for many reasons. One important reason is related to the question of where to find the position of the temperature maximum. As the steam evacuates both forwards (towards the periphery of the segments) and backwards (towards the inlet), the position can be seen as a stagnation point, which implies a zero pressure gradient,  $\partial P/\partial r$ , see Fig. 2, which shows two temperature profiles for a CD82 refiner.

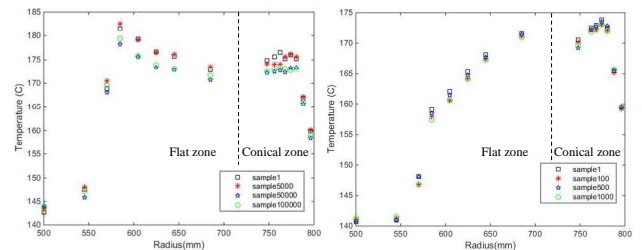


Fig. 2: Temperature profiles at two different test trials and the same type of refining segments. Plots spread over 1000 samples (seconds) in a CD82 refiner.

The stagnation points depend on the type of refining segments used; Sometimes two stagnation points are obtained in a CD refiner, see Fig. 2.

Although the stagnation points in CD refiners are sometimes overlooked in the literature, it turns out that they are vital when deriving both backward and forward flowing steam. It is especially important to stabilize the position of the maximum temperature when running low energy segments to avoid large steam fluctuations in the refining zone and the feeding position in the inlet. This might be considered obvious but temperature profiles are often not available for more advanced refiner control, which makes it difficult to foresee fiber pad fluctuations by only studying the specific energy variations, see Fig. 3. This will be discussed in detail in the appendix.

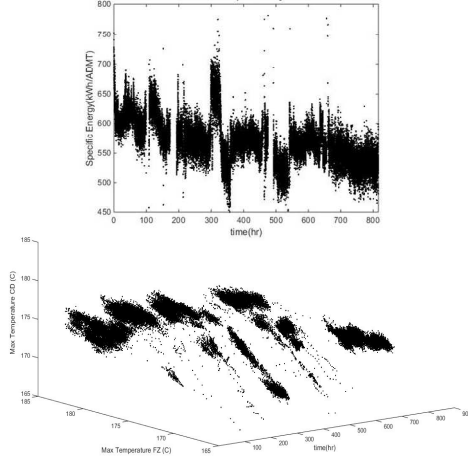


Fig. 3: Upper figure: Specific energy vs. time. Lower figure: Temperature in FZ and CD vs. time.

When modeling refining zone conditions, the position for the stagnation point also becomes important as the steam balance affects a number of internal variables, e.g. the consistency profile.

The extended entropy model is to some extent complex and, in short, the entropy generation can be expressed as

$$dS(r) = m_1 c_p \ln\left(\frac{T(r+dr)}{T(r)}\right) + \sum_{j=2}^3 (m_j(r+dr)s_j(r+dr) - m_j(r)s_j(r))$$

$$w_{th}(r)2\pi r dr = m_1 c_p (T(r+dr) - T(r)) + \sum_{j=2}^3 (m_j(r+dr)h_j(r+dr) - m_j(r)h_j(r))$$

which gives

$$\frac{w_R(r)}{T(r)} 2\pi r dr = m_1 c_p \ln\left(\frac{T(r+dr)}{T(r)}\right) + \sum_{j=2}^3 (m_j(r+dr)s_j(r+dr) - m_j(r)s_j(r))$$

$$m_2(r) + m_3(r) = m_2(r+dr) + m_3(r+dr)$$

$$w_R \neq 0 \text{ and } q_{loss} \approx 0$$

$$m_1^{in} = m_1^{out} = m_1, \quad m_2^{in} \text{ and } m_3^{in} \text{ are known} \Rightarrow$$

$$m_2^{in} + m_3^{in} = m_2^{out} + m_3^{out} \Rightarrow m_2^{out} = m_2^{in} + m_3^{in} - m_3^{out}$$

$$dr = r_{out} - r_{in}$$

Find  $m_3^{out}$ ,  $w_{th_{in}}$  and  $w_{def_{in}}$

$$X = \frac{w_{R_{in}}}{T_{in}} 2\pi r_{in} dr - m_1 c_p \ln\left(\frac{T_{out}}{T_{in}}\right) - m_2^{in}(s_2^{out} - s_2^{in}) - m_3^{in}(s_2^{out} - s_3^{in})$$

$$Y = m_1 c_p (T_{out} - T_{in}) + m_2^{out} h_2^{out} - m_2^{in} h_2^{in} + m_3^{out} h_3^{out} - m_3^{in} h_3^{in}$$

$$m_3^{out} = X / (s_3^{out} - s_2^{out})$$

$$w_{th_{in}} = Y / (2\pi r dr)$$

$$w_{def_{in}} = w_{R_{in}} - w_{th_{in}}$$

Table 1: Latin symbols

Symbol	Description
$c_p$	Heat capacity
$dS$	Entropy generation
$h_i$	Specific enthalpy of component $i$
$m_i$	Material of component $i$
$q_{loss}$	Energy losses per unit area
$r$	Radial coordinate
$s_i$	Specific entropy of component $i$
$S$	Total entropy
$T$	Temperature
$w_{th}$	Thermodynamic work per unit area
$w_{def}$	Refining work per unit area
$w_R$	Estimated total work per unit area

Table 2: Greek symbols

Symbol	Description
$\delta$	Viscous dissipation
$\mu$	Dynamic viscosity
$\omega$	Angular speed of the refiner disc
$\Delta$	Plate gap at radius $r$

Table 3: Indices

Sub-&Superscript	Description
$1$	Wood/Pulp phase
$2$	Water phase
$3$	Steam phase
$in$	Refiner inlet
$out$	Refiner outlet

As seen above, this gives the defibration work,  $w_{def}$ , and thermodynamical work,  $w_{th}$ , in the refining zone, and it is the knowledge of the mass flows of pulp ( $m_1$ ) and water ( $m_2$ ) as a function of the radius that provides the possibility to derive the consistency profile in the refining zone as

$$C(r) = m_1 / (m_1 + m_2)$$

The model was verified by Karlström et al. (2015, 2016a,b) for a number of test series in a full-scale CD82 refiner, see Fig. 4. This gave the possibility to even further analyze different process conditions related to other internal variables such as distributed defibration work, forces obtained when fibers interacted with the bars and grooves in the refining zone.

To fully understand the modeling efforts when deriving soft sensors, it is important to model geometrical properties as well. Even though such properties, in terms of refining segment patterns, directly affect the shape of

the temperature profile, the position of the contraction of the refining segments plays a vital role from a geometrical perspective. Moreover, this position indicates how much the shear force will change under certain conditions, and Karlström and Eriksson (2014a,b) showed that this was not well described. They showed that the plate gap,  $\Delta_{gap}$ , which is measured in one radial position along the radius, is not sufficient as an input and that information is needed about the radially dependent distance between the refining segments,  $\Delta(r)$ , which also include the taper  $\Delta_{taper}(r)$ , see Fig. 5.

Hence, according to Fig. 5, the distance between the refining surfaces can be expressed as

$$\Delta(r) = 2\Delta_{taper}(r) + \Delta_{gap}$$

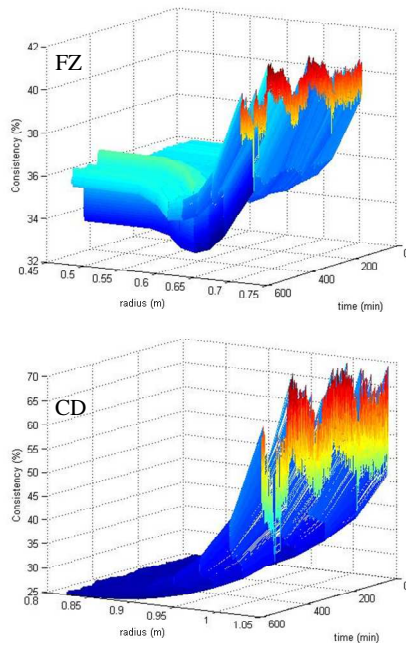


Fig. 4: Typical consistency profiles in the FZ and CD zones as functions of radial position and time.

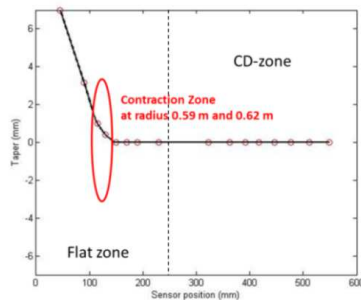


Fig. 5: The taper,  $\Delta_{taper}(r)$ , describing one side of the segments in the flat zone and CD zone, respectively. Note that the plate gaps,  $\Delta_{gap}$ , in the flat zone and the CD zone are not included in this figure.

As indicated above, the geometrical perspective in terms of the segment pattern must also be considered in the model as it clearly influences the refining conditions and thereby the process performance. The effective cross sectional surface, see Fig. 6, must therefore be included when deriving physical variables in the refining zone.

There is a large variety in segment design parameters, and variations in patterns along the radius must be considered in the model as they affect e.g. the pulp residence time as well as the fiber development itself. The bar density is set to

$$\eta(r) = B(r)/(B(r) + G(r))$$

where  $B(r)$  and  $G(r)$  are vectors and define the bar and groove width along the radius of the refining segments. It is obvious that the bar density must be considered when describing the cross-sectional area that is available for the fibers on their path from any position along the radius to the periphery of the segments.

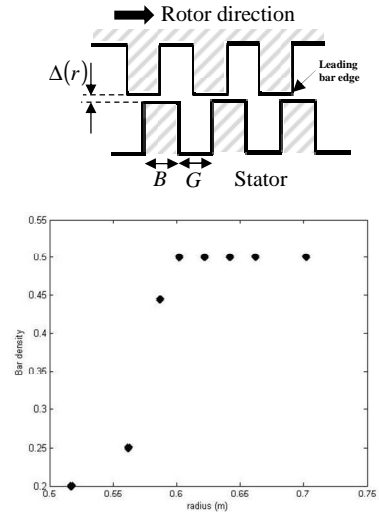


Fig. 6: Upper: Cross section of a hypothetical refiner segment. Lower: Bar density for typical segments in a CD refiner.

In the literature, the fiber residence time  $\tau$  is exclusively related to the pulp without considering the effect of chip, pulp, and fiber interaction with steam and free water (at the beginning of the refining zone). Karlström and Eriksson (2014a,b) commented on this point, but the theory was only vaguely linked to the residence time via the chip, pulp and fiber viscosity variations. To simplify the description, we prefer to describe the residence time as the fiber residence time, i.e. the average transport time of fibers from the inner part of the refining zone to the outside rim of the refining segments

$$\tau = \int_{r_{in}}^{r_{out}} \frac{1}{v_1(r)} dr = \int_{r_{in}}^{r_{out}} \frac{\rho_1(r) A_1}{m_1(r)} dr$$

The density,  $\rho_1$ , mass flow,  $m_1$ , cross-area available for the pulp,  $A_1$ , and residence time,  $\tau$ , between arbitrary positions in the refining zone  $\{r_{in}, r_{out}\}$  can therefore be estimated as well. The volumetric flows must be considered to find the cross-area available for the pulp,  $A_1$ . The steam flow,  $V_3$ , is much larger than the volumetric flows of pulp  $V_1$  and water  $V_2$  together, i.e.  $abs(V_3) \gg (V_1 + V_2)$ . In the extended entropy model it is shown that the vapor velocity,  $v_3$ , is much larger than the pulp velocity,  $v_1$ , in the refiner, see Karlström and Hill

(2014a). As a result, the vapor is assumed to diffuse faster into the grooves as compared with the pulp due to the tangential pressure drop and the radial pressure drop. The interplay between the tangential and radial pressure gradients is complex, but it is important to stress when discussing intricate fluid dynamics between the refining segments; here it is assumed that the volumetric steam flow is primarily localized at the grooves. The major part of the moving pulp, including the bounded water, will thereby be localized to the cross-sectional area between the bars and a hypothetical boundary layer between the stator and the rotor where the steam flow is not dominant.

From the assumption  $v_1(r)=v_2(r)$ , the cross-sectional area for the water will be  $A_2=A_1V_2/V_1$ . Knowing the refining segment geometry, we also know the total cross-sectional area,  $A_{TOT}$ . The total volumetric flow,  $V_{TOT}$ , is known from the extended entropy model, see the discussion above. Together with the derived vapor velocity, which is much larger than the pulp velocity, i.e.  $v_3(r) \gg v_1(r)$ , the cross-sectional area for the vapor can be derived.

$$A_1 = \frac{V_1}{V_1 + V_2} (A_{TOT} - A_3)$$

$$A_3 \ll \frac{V_3}{V_1} A_1 = \frac{V_3}{V_1 + V_2} (A_{TOT} - A_3) \Rightarrow A_3 \left( \frac{V_{TOT}}{V_1 + V_2} \right) \ll \frac{V_3}{V_1 + V_2} A_{TOT}$$

$$A_3 \ll \frac{V_3}{V_{TOT}} A_{TOT}$$

However,  $V_3 \approx V_{TOT}$ , which means that  $A_3 \ll A_{TOT}$ , i.e.

$$\begin{cases} A_{1_{FZ}} \approx \frac{V_{1_{FZ}}}{V_{1_{FZ}} + V_{2_{FZ}}} A_{TOT_{FZ}} \\ A_{1_{CD}} \approx \frac{V_{1_{CD}}}{V_{1_{CD}} + V_{2_{CD}}} A_{TOT_{CD}} \end{cases}$$

## Results and discussion

There is no doubt that the temperature measurements can be seen as internal variables measured inside the refining zone. Such measurements together with traditional process variables, such as dilution water flows, plate gaps and specific energy are vital in terms of spanning the material and energy balances. The traditional process variables are consequently called external variables as they are measured outside the refiner or, like the plate gaps, can be classified as not typical physical phenomena<sup>1</sup>.

To summarize, we can conclude that using a model that describes the major physical phenomena in a refining zone provides a possibility to predict several other internal variables such as:

- Fiber residence time (which is actually possible to define spatially dependent on segment pattern etc.);
- Consistency profile (which can be used as vector or divided into scalars such as  $C_{FZout}$  and  $C_{CDout}$ );

- Forces on bars (see Karlström and Eriksson (2014a,b) for details);
- Defibration work and thermodynamic work (which is important for the entire steam balance);
- Back-flowing steam (which can be used in future algorithms to predict incoming chip moisture);
- Pulp, water velocity and steam velocity (vital when analyzing e.g. feeding problems at different production levels).

As seen above, the extended entropy model is not a dynamic model based on partial differential equations. This was motivated by Karlström et al. (2008) as a consequence of the extremely fast dynamics in the refining zone (ranging from 0.5 to 1 second) together with the slower actuator dynamics for plate gap changes and the overall dominant dynamics in the inlet and outlet piping. All this limits the possibilities to control the refiner fast enough to cope with the instant refining zone dynamics, see the further discussion in Karlström and Hill (2014a,b, 2015a,b). However, the combination of fast and slow dynamics also opens the possibility for a robust on-line implementation of the equations described above. It is valuable to stress this. Nevertheless, the model derived above must be further developed to become a useful tool for on-line analysis and future control applications. To expand the model to cover most of the equipment surrounding a refiner, we introduce different blocks as illustrated in Fig. 7.

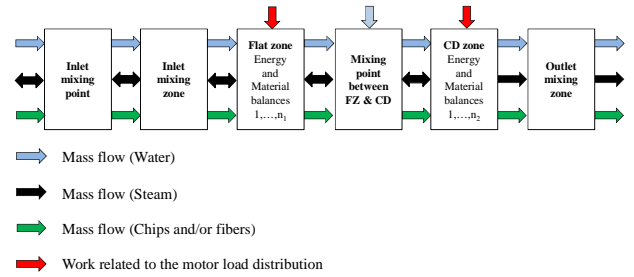


Fig. 7: Schematic description of the material and energy balances spanning the CD refiner.

Hence, in the complete model, the following information can be added:

- **Inlet mixing point** is the position where wood chips meet dilution water added to the inlet zone.
- **Inlet mixing zone** corresponds to the zone close to the flat zone, where the inlet pressure of possible added steam meets the chips and water.
- **Flat zone (FZ) energy and material balances 1,..., n1**: The blocks describing energy and material balances in the flat zone.  $n_1$  sensors are assumed.
- **Mixing point between flat zone and CD zone**: The dilution water added to the CD zone will be a central variable as it is vital for the distributed work and for the consistency estimations.
- **CD zone energy and material balances 1,..., n2**: The blocks describing energy and material balances in the CD zone.  $n_2$  sensors are assumed.

<sup>1</sup> In this context, the specific energy is also classified as an external variable even though the motor load, which is the integral of all work distribution in the refining zone, can be seen as an internal variable.

- **Outlet mixing zone:** The mass flows in the CD zone meet in this position of the refiner casing. Most often this zone is associated with a flash calculation, as the temperature and pressure are normally lower in this position compared with inside the CD zone.

It is important to mention that the block called “Mixing point between FZ & CD” corresponds to the position in the refining zone where dilution water is added to the CD zone. This is a schematic illustration and, in several CD refiners, the dilution water is added distributed over the middle section of the segments, which must be considered when using the models as soft sensors.

This paper focuses on the process conditions and how to use the model to provide new information about properties (internal variables) that are not possible to measure. Here, the consistency out from the flat and conical zones will be considered together with corresponding fiber residence times in the refining zones.

To illustrate how to use internal variables for process analysis, the test according to Fig. 8 was performed.

Initially, it was difficult to increase the production, and manipulation of the plate gap and dilution water to the CD zone were too risky in a pulp quality perspective.

As the main target was to increase the production rate, the operators had to open the plate gap in the conical zone at the same time as the plate gap was reduced in the flat zone. In other words, a better refiner controllability was provided.

The operators requested more information about the process conditions in the flat zone before changing the operating point; to overcome that problem, the extended entropy model was used before and after each step change in the plate gap, dilution water feed rate and production.

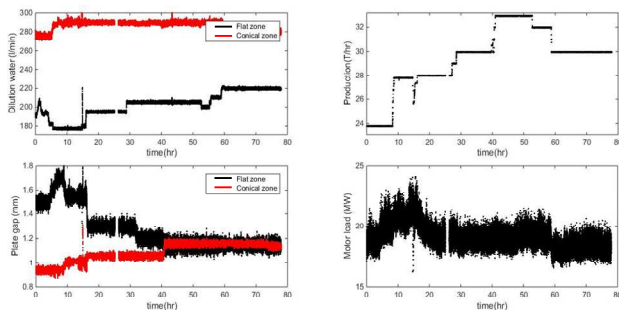


Fig. 8: Step changes performed in the external variables of dilution water (upper left), production (upper right) and plate gap (middle left); response in motor load including time for each test point (middle right).

Besides the information about the temperature profile changes at different process conditions, the use of the model provided information about fiber residence times in each refining zone and consistency profile, as well as the motor load split in the refiner, see Fig. 9 and Fig. 10. The strategy to distribute more work to the flat zone compared with the conical zone (at the same time as the consistencies in each zone were followed closely) opened the possibility for an increased production rate.

It is interesting to see that the motor load in Fig. 8 is not affected so much when more work is applied to the flat

zone, which also indicates that the split was not optimized before the test.

In short, the idea in the test can also be illustrated by showing the ratios between the plate gaps, dilution water feed rates and consistencies in FZ and CD besides the maximum temperatures, see Fig. 11, when the production rate is increased.

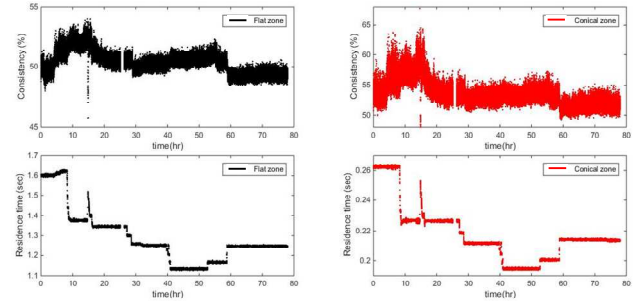


Fig. 9: Upper left and right: Responses in the consistencies out from FZ and CD. Lower left and right: Residence times in FZ and CD.

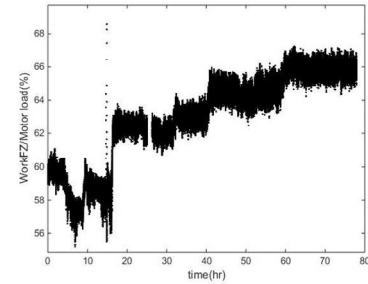


Fig. 10: Ratio between the estimated work in the flat zone and the total motor load.

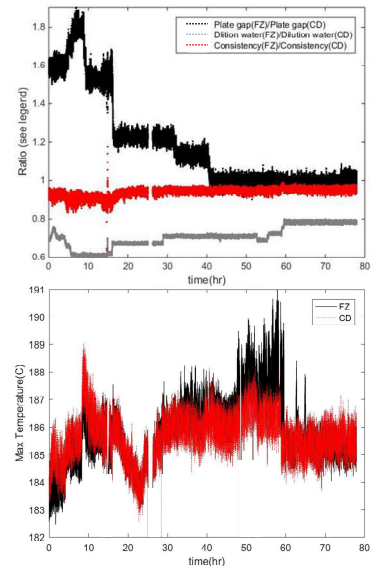


Fig. 11: Upper figure: The ratios between selected external and internal variables in the flat zone and conical zone. The ratios highlight the strategy to keep a stable consistency ratio when running the test according to Fig. 8. Lower figure: Temperature maximum in FZ and CD, respectively.

As seen in Fig. 11, the temperature maximum position can fluctuate dramatically depending on different process conditions. This was also indicated in Fig. 2, but, in Fig. 12, the temperature profile is flatter which means that the

position of the zero pressure gradient,  $\partial P/\partial r=0$ , can vary and thereby cause fluctuating backward and forward flowing steams. This is not an optimal situation and calls for further attention in future control applications, see the appendix.

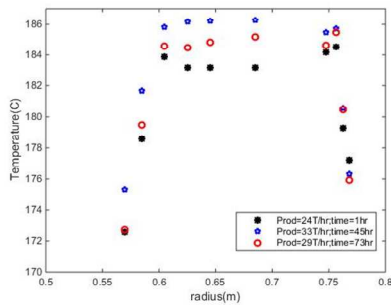


Fig. 12: Temperature profiles (three production levels) in a CD82 refiner.

To verify the consistency estimation using the extended entropy model, manual tests were made in the blow-line out from the refiner, see Fig. 13. Note that, without the model, the internal variables in the flat zone are impossible to estimate. This is a huge step forward in the development of different control strategies for CD refiners in general.

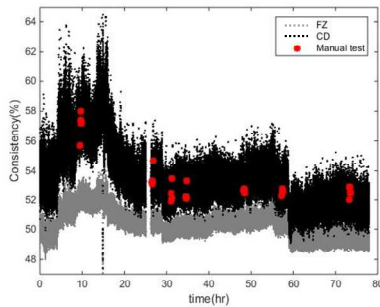


Fig. 13: Estimated consistencies out from the flat and conical zones together with manual consistency derived from samples in the blow-line.

Finally, as the motor load during the test was relatively stable, see Fig. 9, at the same time that the production could be increased from 24 to 33 ADMT/hr, the specific energy demand was ultimately reduced dramatically, by about 40%, see Fig. 14<sup>2</sup>. This also led to a situation where two small refiners could be closed down without violating the pulp and handsheet property specification

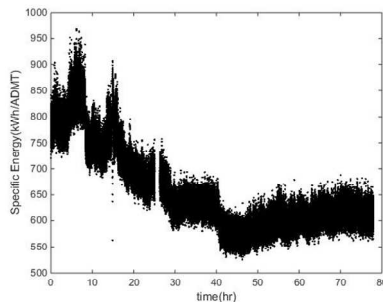


Fig. 14: Specific energy reduction when following the procedure outlined.

<sup>2</sup> Similar results from a Jyhla SD65 refiner have been published earlier by Harkonen and Tienveri (1995).

When increasing the production rate, it is always important to check the pulp specification in terms of the amount of shives in the sample. As seen in Fig. 15, both the long and wide measures for shives increase slightly. However, by tuning the consistency together with the temperature profile in the flat and conical zones, the increased shives can be reduced to normal levels. This was not performed during the test as the pulp specification was met.

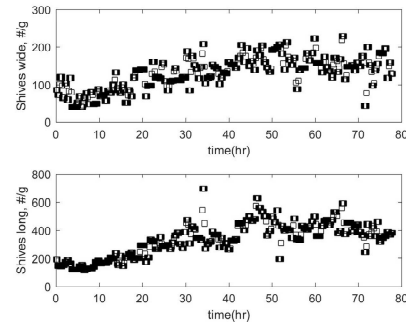


Fig. 15: Wide and long shives versus time.

## Concluding remarks

The main purpose of this study is to study how the internal variables (e.g. temperature, consistency, fiber residence time, backward flowing steam and forces obtained when fibers interact with the refining bars) can be used and analyzed in different parts of the refining zones. It is shown how they differ from the traditional external variables (e.g. dilution water feed rate, specific energy and plate clearance).

The internal variables turn out to be invaluable when trying to optimize the refining process, develop new refining segment patterns etc. and they can be seen as the backbone of physical models of CD-82 refiners. Moreover, such models can be used for on-line implementation of soft sensors where the internal variables open a new set of opportunities for extended control concepts.

To keep track of the fiber development, it is important to stabilize the backward flowing steam. That is done in the work here by stabilizing the temperature profile. When the temperature profile is stabilized, both the fiber residence time and the consistency profile must be optimized to maintain the pulp quality variations within a pre-specified interval. This is illustrated in this paper by a test performed to maintain the ratio between the consistencies out from the flat and conical zones stable when increasing the production rate.

It is furthermore shown that the production rate together with the plate gaps have a considerable effect on the fiber residence time, which must be studied in more detail to minimize e.g. an increased shives content. In other words, both the fiber residence times and the consistencies in the flat and conical zones are important internal variables that affect the pulp development when optimizing the process. This will be analyzed in coming papers in this series.

In summary, we can conclude that it is possible to optimize the process to meet a 40 % specific energy

reduction without violating the pulp property specification.

---

### Acknowledgements

The authors gratefully acknowledge the funding of the Swedish Energy Agency, StoraEnso and Holmen Paper. Special thanks go to the StoraEnso Skoghall mill and Lars Johansson (Paper and Fibre Research Institute), for running trials and providing the excellent laboratory and process data used in this study.

---

### Literature

- Berg, D.** (2005): A Comprehensive Approach to Modeling and Control of Thermomechanical Pulping Processes, Lic thesis. Dept. of Signals and Systems, Chalmers.
- Bird, R.B., Stewart W.R. and Lightfoot, E.N.** (1960): Transport phenomena, John Wiley and Sons Inc., New York.
- Backlund, H.-O., Höglund, H. and Gradin, P.** (2003): Study of tangential forces and temperature profiles in commercial refiners, Int. Mech. Pulping Conf., Quebec, Canada, 2-5 June 2003, PAPTAC, Montreal, Canada, pp. 379-388.
- Dahlqvist G. and Ferrari B.** (1981) Mill operating experience with a TMP refiner control system based on a true disc clearance measurement, Int. Mech. Pulping Conf., Oslo, Norway, Session III, no. 6.
- Eriksson, K.** (2005): An Entropy-based Modeling Approach to Internally Interconnected TMP Refining Processes, Licentiate thesis, Chalmers University of Technology, Göteborg, Sweden. University of Technology, ISSN 1403-266x; nr R034/2005.
- Eriksson, K.** (2009): Towards improved control of TMP refining processes, PhD thesis, Chalmers University of Technology, Göteborg, Sweden.
- Harkonen, E., Tienverri, T.** (1995): The influence of production rate on refining in a specific refiner. Int. Mech. Pulp. Conf. Ottawa, Canada p. 177.
- Harkonen, E., Huusari, E. and Ravila, P.** (1999): Residence time of fibre in a single disc refiner, International Mechanical Pulping Conference, Houston, USA.
- Harkonen E., Kortelainen J., Virtanen J., Vuorio P.** (2003): Fiber development in TMP main line. International Mechanical Pulping conference, Quebec, Que, Canada, 2-5 June 2003, pp 171-178.
- Hill, J., Westin, H., and Bergstrom, R.** (1979) Monitoring pulp quality for process control, Int. Mech. Pulping Conf., Toronto, Canada, p. 111-125.
- Hill, J., Saarinen, K., Stenros, R.** (1993) On the control of chip refining systems, Pulp and Paper Canada, 94(6), p. 43-47.
- Honkasalo, J.V., Polkkynen, E.E., Vainio, J.A.,** (1989) Development of control systems in mechanical pulping (GW, TMP) at Rauma, Int. Mech. Pulping Conf., Helsinki, Finland, p. 376-389
- Johansson B.-L., Karlsson H., Jung, E.,** (1980) Experiences with computer control, based on optical sensors for pulp quality, of a two-stage TMP-plant, 1980 Process Control Conf., Halifax, Nova Scotia, p. 145-152.
- Karlström, A., Berg, D. and Eriksson, K.** (2005): Developments in soft sensors for measurement of refining parameters, Scientific and technical advances in refining and mechanical pulping, Barcelona, Spain, 28 Feb.-4 Mar. 2005, Pira International, Leatherhead, UK, Paper 5.
- Karlström, A., Eriksson, K., Sikter, D. and Gustavsson, M.** (2008): Refining models for control purposes, Nord. Pulp Paper Res. J 23(1), 129.
- Karlström, A., and Isaksson, A.** (2009): Multi-rate optimal control of TMP refining processes, Int. Mech. Pulping Conf., Sundsvall, Sweden.
- Karlström, A.,** (2013): Multi-scale modeling in TMP-processes, 8<sup>th</sup> Int. Fundamental Mech. Pulp Res. Seminar, Åre, Sweden.
- Karlström, A. and Eriksson, K.** (2014a): Refining energy efficiency Part I: Extended entropy model. Nord. Pulp Paper Res. J. 29(2).
- Karlström, A. and Eriksson, K.** (2014b): Refining energy efficiency Part II: Forces acting on the refining bars. Nord. Pulp Paper Res. J. 29(2).
- Karlström, A. and Eriksson, K.** (2014c): Refining energy efficiency Part III: Modeling of fiber-to-bar interaction. Nord. Pulp Paper Res. J. 29(3)
- Karlström, A. and Eriksson, K.** (2014d): Refining energy efficiency Part IV: Multi-scale modeling of refining processes. Nord. Pulp Paper Res. J. 29(3).
- Karlström, A. and Hill J.** (2014a): Refiner Optimization and Control Part I: Fiber residence time and major dynamic fluctuations in TMP refining processes. Nord. Pulp Paper Res. J. 29(4).
- Karlström, A. and Hill J.** (2014b): Refiner Optimization and Control Part II: Test procedures for describing dynamics in TMP refining processes. Nord. Pulp Paper Res. J. 29(4)
- Karlström, A. and Hill J.** (2015a): Refiner Optimization and Control Part III: Natural decoupling in TMP refining processes. Nord. Pulp Paper Res. J. 30(3).
- Karlström, A., Eriksson, K. and Hill J.** (2015b): Refiner Optimization and Control Part IV: Long term follow up of control performance in TMP processes. Nord. Pulp Paper Res. J. 30(3).
- Karlström, A., Hill J., Ferritsius, R. and Ferritsius, O.** (2015): Pulp Property Development Part I: Interlacing Undersampled Pulp Properties and TMP Process Data using Piece-wise Linear Functions. Nord. Pulp Paper Res. J. 30(4), 599-608.
- Karlström, A., Hill J., Ferritsius, R. and Ferritsius, O.** (2016a): Pulp Property Development Part II: Process Nonlinearities and its Influence on Pulp Property Development. Submitted for publication in Nord. Pulp Paper Res. J.
- Karlström, A., Hill J., Ferritsius, R. and Ferritsius, O.** (2016b): Pulp Property Development Part III: Fiber Residence Time and Consistency Profile Impact on Specific Energy and Pulp Properties. Submitted for publication in Nord. Pulp Paper Res. J.
- Kure, K.-A** (1999): On the relationship between process input variables and fiber characteristics in thermomechanical pulping, PhD thesis 45:99, Norwegian Univ. Science and Technology, Trondheim.
- Kerekes, R.J. and Senger, J.J.** (2006): Characterizing Refining Action in Low Consistency Refiners by Forces on Fibres, J. Pulp Paper Sci., 32(1), 1-8.
- Kerekes, R.J.** (2011): Force-based characterization of refining intensity, Nord. Pulp Paper Res. J., Vol 26 no. 1.
- Lehtonen, S., Virtanen, P., Lindeberg, M., Fralic, G. A.,** (2014): New TMP optimization approach: using advanced quality control to stabilize tensile strength and reduce power cost. International Mechanical Pulping Conference, Helsinki, Finland.



Lundin, T., Batchelor, W., Fardim, P. (2008): Fiber Trapping in Low Consistency Refining: New Parameters to Describe the Refining Process, Tappi J., 15-21, July, 2008.

Miles, K. B. and May, W. D. (1990): The Flow of Pulp in Chip Refiners, J. Pulp Paper Sci. 16(2), 63.

Miles, K. B. and May, W. D. (1991): Predicting the performance of a chip refiner: A constitutive approach, Int. Mech. Pulping Conf. p 295-301.

Murton, K., Duffy, G., Corson, S. (2002): Pulp residence time influence on refining intensity and pulp quality, Proceedings of 56<sup>th</sup> Appita Annual Conference, Carlton, pp. 185-193.

Oksum J., (1983) New technology in the Skogn mechanical pulp mill, Int. Mech. Pulping Conf., Washington DC, USA, p. 143-153.

Sabourin, M., Wiseman, N. and Vaughn, J. (2001): Refining theory considerations for assessing pulp properties in the commercial manufacture of TMP. 55<sup>th</sup> Appita Annual Conference, p 195-204.

Senger, JJ., Siadat, A., Ouellet, D. and Wild, P. (2004): Measurement of normal and shear forces during refining using a piezoelectric force sensor, J. Pulp Paper Sci., vol 30 no. 9.

Strand, B.C., Mokvist, A., Falk, B., Jackson, M. (1993): The effect on production rate on specific energy consumption in high consistency chip refining, IMPC 1993, pp. 143.

Strand, B.C. (1996): Model based control of high consistency refining, TAPPI Journal 79(10), pp.140-146.

Strand, B.C., Grace, B. (2014): Implementation of advanced supervisory control within a TMP refiner quality control system, International Mechanical Pulping Conference, Helsinki, Finland.

## Appendix

When changing the refining segments from a standard pattern to a low energy segment characterized by another type of pattern including a larger taper, see Fig. 16, we expect to find another type of temperature profile. No complete description of the segment parameters will be included in the text of this appendix. However, all required parameters related to the description in the main text are included in the extended entropy model.

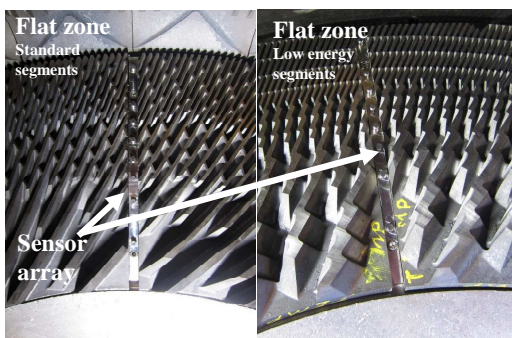


Fig. 16: Left figure: Standard segments in FZ. Right figure: Low energy segments in FZ.

As indicated earlier, the temperature profile can be rather flat when the refiners are run at different operating conditions. This is true for standard segments but is perhaps even more pronounced when using low energy segments. This complicates the stabilization of the

process, and we will in this appendix illustrate what happens with the back-flowing steam when running at different operating conditions.

Even though dynamic effects on the refining stability have been discussed for decades, it is obvious that this knowledge has been overlooked in daily process operations. Consider the test procedure according to Fig. 17, where standard segments according to Fig. 16 are used. The test was performed using three distinct sets of different chip mixtures (TEST1: 100% saw mill; TEST2: 65% saw mill and 35% roundwood; and TEST3: 100% roundwood.) to define a relatively large operating window.

According to Fig. 18, the position where we expect to find the temperature maximum in the flat and conical zones does not change dramatically, i.e. the zero pressure gradient,  $\partial P/\partial r=0$ , is spatially stable at the 8<sup>th</sup> position in the flat zone.

The stable position for the maximum temperature means that the estimated back-flowing steam is expected to be stable as well, see Fig. 19.

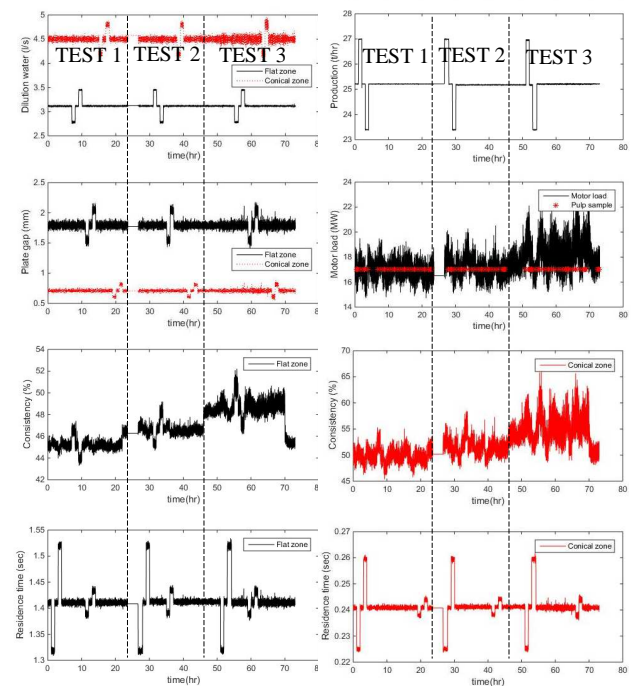


Fig. 17: Step changes performed in the external variables of dilution water (upper left), production (upper right) and plate gap (middle left); response in motor load including time for each test point (middle right). Responses in the internal variables of consistency and residence time (lower figures).

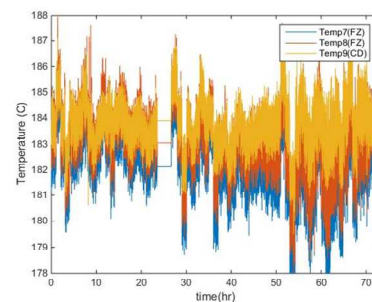


Fig. 18: Three selected temperatures at the end of the flat zone and the beginning of the conical zone when using the standard segments described in Fig. 16.

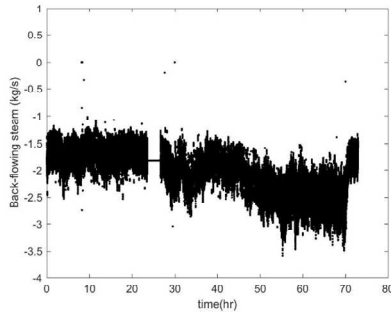


Fig. 19: Estimated back-flowing steam when performing the test according to Fig. 17.

When running low energy segments, according to the test in Fig. 8, a completely new situation occurs with a temperature profile that is most often flat at the temperature maximum, see Fig. 12. This means that we can expect fluctuations in the position for the maximum temperature. This is confirmed in Fig. 20, where the temperatures at the “flat region” are shown.

The fluctuations in the position of the temperature maximum correspond to about an 80-mm shift and significantly affect the amount of back-flowing steam, see Fig. 21.

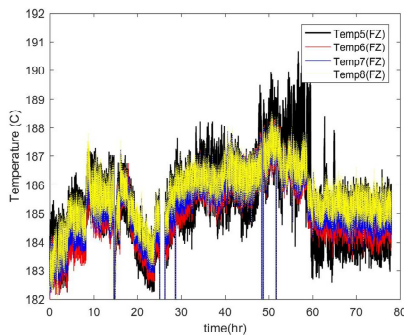


Fig. 20: Four selected temperatures at the end of the flat zone when using the standard segments described in Fig. 16.

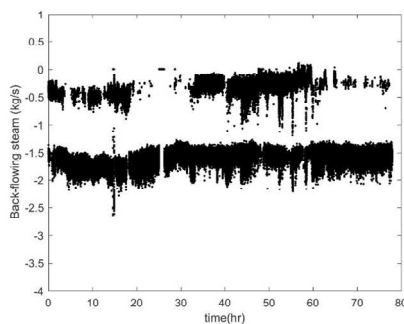


Fig. 21: Estimated back-flowing steam from the flat zone when performing the test according to Fig. 17.

It is not only the back-flowing steam will be affected by the pulsations obtained when the steam turning point change position; the forward-flowing steam will be affected as well, see Fig. 22.

By taking into account all aspects regarding pumping effects backwards and forwards, we end up in a rather complex analysis, which certainly can affect the pulp quality negatively. To avoid such situations and get a better fiber pad stabilization, it is wise to reduce the plate

gap in the flat zone, in this specific situation, to stabilize the temperature profile. Note that, in other parts of the refining operating window, another situation can be obtained. However, the temperature profile will still guide the operator to take the proper action.

An extension to stabilize the temperature profile by changing the plate gap was not performed during the test. This is of course a natural next step when implementing advanced control systems for energy and pulp property optimization.

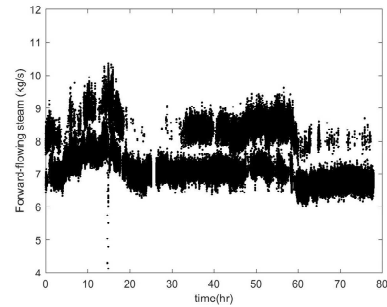


Fig. 22: Estimated forward-flowing steam out from the conical zone when performing the test according to Fig. 17.

In the research literature related to the development of the extended entropy model, it can be concluded that the irreversible work or the defibration/fibrillation work can fluctuate significantly along the refining zone radius in CD82 refiners. The results were obtained from TMP data, see Karlström and Eriksson (2014a,b,c,d), and it was concluded that all variables and parameters, significant for the type of refiner, must be included in the model to get a proper estimate of the forces distributed between the refining segments.

Note that the force vector must be derived from the refining work per unit area,  $w_{def}$  as described by the equation set in the main text and not the total work, including the thermodynamical work, which is common practice when only the specific energy is available as an external variable. This is motivated from the fact that only a fraction of the thermodynamical work will contribute to the viscous dissipation. Moreover, it has been shown that the magnitude of forces on each bar coincides with the measured fiber-to-bar interaction, see Backlund et al. (2003) and Senger et al. (2004), if the defibration/fibrillation work is considered and not the total work related to the motor load (or specific energy), see Karlström and Eriksson (2014a,b,c,d).

Karlström and Eriksson (2014b) also showed that the distributed forces obtained from the interaction between fibers and bars vary a great deal depending on operating conditions, which resulted in the statement that

*“the refining intensity as defined by Miles and May (1990, 1991), Kerekes and Senger (2006), Kerekes (2011) and Lundin et al. (2008) should be developed further and not be considered as a scalar nor estimated based on assumed effective coefficients of friction”.*

In this paper it is of special interest to study the force distribution related to the fiber-to-bar interaction, especially when

- changing the production rate as described above in Fig. 8;
- the back-flowing steam varies according to Fig. 21.
- Estimating the average forces on each bar at different positions in the refining zone at different production levels is straightforward, following the equations outlined in the main text, see Fig. 23.

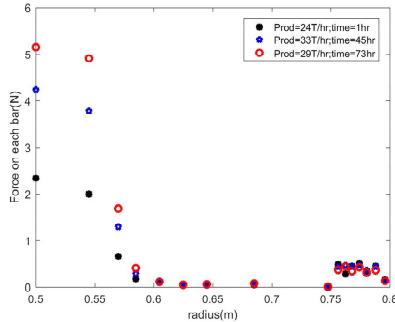


Fig. 23: Distributed forces, averaged over one hour, along the refining zone radius when changing the production rate according to Fig. 8.

It is interesting to see in Fig. 23 that the forces are quite dominant in the inner part of the flat zone, which is a result of the bar width for refiner segments in Fig. 16. The forces on each bar rapidly decrease thereafter to levels similar to those described by Karlström and Eriksson (2014a,b,c,d). As the morphology of the pulp changes along the radius, the first fiber-to-bar impact will be essential and differ depending on the production level. Describing the refining intensity as a scalar should also be questioned in this situation.

The varying back-flowing steam as described in Fig. 21 will of course also affect the fiber-to-bar interaction according to Fig. 24. Two distinct profiles<sup>3</sup> will be obtained when running at the highest production rate (33 T/hr), which will certainly affect the development of the pulp quality. It is interesting to note that the forces in the inner part of the refining zone vary more than 40 % for this specific production level<sup>4</sup>.

<sup>3</sup>When the back-flowing steam is high, the steam and fiber balance will result in larger forces on each bar. This is a consequence of the higher local work when the back-flowing steam increases.

<sup>4</sup>When comparing the results in this paper with previous results from a CD82 TMP refiner (Karlström and Eriksson (2014a,b,c,d)), a number of different aspects can be discussed. One significant difference is that the maximum force is obtained at the 3<sup>rd</sup> sensor due to the specific refining segment pattern used. Another important issue is related to the difference in bar width when comparing the two cases. The refining segments in this CTMP process have a larger bar width in the inner part of the segments compared with the “TMP segments” studied in Karlström and Eriksson (2014a,b,c,d), which means that the forces on each bar become larger and can cause segment erosion. This even more stresses the need to include the segment parameters when modeling refining conditions in general to foresee possible risks for segment wear.

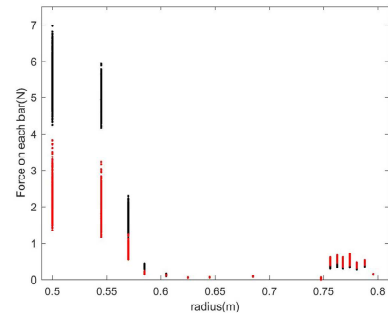


Fig. 24: Forces distributed on each bar, along the refining zone radius at a stable production level with varying back-flowing steam (red dots correspond to less back-flowing steam).

To summarize, we can conclude that the traditional measure of refining intensity is questioned as the fiber-to-bar impact is strongly dependent on the refining segment pattern and how long the fibers on average stay in different parts of the refining zone. The segments are characterized by different lengths, widths and depths of the bars and grooves, which are all essential features to cope with.

We can make an assumption that the residence time is divided into two parts, one that describes the time for fiber-to-bar impact between sensor 1 and sensor 4 and one describing the time for fiber-to-bar interaction between sensor 4 and sensor 8 in the flat zone.

The fiber residence time is an internal variable that can be studied in different intervals along the radius. If the ratio between these variables is constant, we can expect to find a similar refining intensity at different process conditions. As seen in Fig. 25, this is of course not the case, and the fibers stay much longer in the central parts of the flat zone (sensors 1-4) compared with the outer flat zone (sensors 4-8) when increasing the production according to Fig. 12 and the test procedure described in the main text.

The results presented in this paper offer new on-line applications where the distributed force vector can be used as an internal variable together with residence time, consistency etc. when analyzing the refining performance. This will be discussed further in coming papers where the external and internal variables impact on pulp and handsheet properties will be analyzed in more detail.

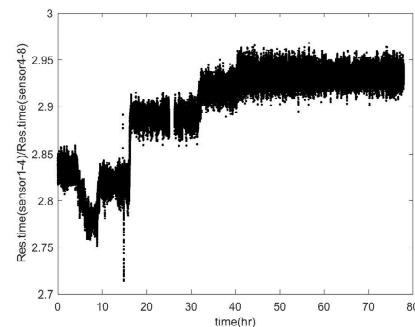


Fig. 25: Residence time ratio between the inner and outer parts of the flat zone.